Fourier-space paths applied to the calculation of diffusion for the Chirikov-Taylor model

A. B. Rechester
Plasma Fusion Center, Massachusetts Institute of Technology, Cambridge, Massachusetts 02139

M. N. Rosenbluth*
Institute for Advanced Study, Princeton, New Jersey 08540

R. B. White
Plasma Physics Laboratory, Princeton University, Princeton, New Jersey 08544

(Received 23 June 1980)

A compact path-diagram method has been introduced for the calculation of velocity moments of a probability function. This method is complementary to the approach developed earlier by Rechester and White. It is applied to the Chirikov-Taylor model. Analytic expressions for velocity-space diffusion have been derived and compared with numerical computations. A numerical method for path summations has been developed which is more efficient than directly advancing the model equations, and is applicable for small field-amplitude values, where the direct stepping method is impractical.

I. A PROBABILITY DESCRIPTION FOR EVOLUTION IN PHASE SPACE

The purpose of this work is a further development of a probabilistic method outlined in Ref. 1. As before, we will consider the simple case of charged particles moving in a field of electrostatic plane waves. The equations of motion for the Chirikov-Taylor model are[1-3]

$$x_{t+1}=x_t+v_{t+1}\,, \tag{1}$$

$$v_{t+1}=v_t-\epsilon\sin x_t\,. \tag{2}$$

All variables here are dimensionless, x represents the coordinate and v the velocity, and time t takes on integer values $t=0,1,2,\ldots$. The parameter ϵ is related to the electric-field amplitude. Without loss of generality, we may assume it to be a positive number. We will also assume periodic boundary conditions in x, $0\leq x\leq 2\pi$. Following Ref. 1, we substitute the deterministic description given by Eqs. (1) and (2) with a probabilistic one by introducing an additional random step δx_t in Eq. (1). This variable has a probability distribution given by

$$G(\delta x_t,v_t)=(2\pi\sigma)^{-1/2}\sum_{n=-\infty}^{\infty}\exp\left(-\frac{(\delta x_t-v_t+2\pi n)^2}{2\sigma}\right). \tag{3}$$

Equation (3) can be derived by introducing a diffusion term ($\sigma/2$, the diffusion coefficient) into the Vlasov equation.[1] Let $P(x,v;t)$ be a time-dependent probability function of phase-space points x, v with the initial condition given by

$$P(x,v,o)=\frac{1}{2\pi}\delta(v-v_0)\,. \tag{4}$$

Then according to Eqs. (1)–(3) the time evolution of P in the interval $t-1$, t is given by

$$P(x,v,t)=\int_0^{2\pi}G(x-x',v)\,P(x',v+\epsilon\sin x',t-1)\,dx'\,. \tag{5}$$

The Fourier transformation of this function in x and v can be written as

$$P(x,v,t)=\frac{1}{(2\pi)^2}\sum_{m=-\infty}^{\infty}\int_{-\infty}^{\infty}dk\,a_m^t(k)\exp[i(mx+kv)]\,. \tag{6}$$

From (4) it follows that

$$a_m^0(k)=\delta_{m0}\exp(-ikv_0)\,, \tag{7}$$

where $\delta_{m,n}$ is a Kronecker function. The relation between the Fourier amplitudes $a_m^t(k)$ at times t and $t-1$ can be easily derived from Eqs. (5) and (6) by substituting the identity

$$\exp(\pm iz\sin x)=\sum_{l=-\infty}^{\infty}J_l(z)\exp(\pm ilx),\quad z>0 \tag{8}$$

and eliminating the quadratic expression in the exponent of $G(x-x',v)$ through the use of the further identity

$$(2\pi\sigma)^{-1/2}\sum_{n=-\infty}^{\infty}\exp\left(\frac{-(y+2\pi n)^2}{2\sigma}\right)=\frac{1}{2\pi}\sum_{m=-\infty}^{\infty}\exp(-\tfrac{1}{2}\sigma m^2+imy)\,. \tag{9}$$

We then find

$$a_m^t(k)=\sum_{l=-\infty}^{\infty}J_l(|k'|\epsilon)\exp[-(\sigma/2)m^2]a_{m'}^{t-1}(k')\,. \tag{10}$$

Here J_l are Bessel functions and

$$k'=k+m\,, \tag{11}$$

$$m'=m-l\,\mathrm{sgn}k'\,, \tag{12}$$

and

$$\mathrm{sgn}k=\begin{cases}+1, & k>0\\ -1, & k<0\end{cases}.$$

We introduce now velocity moments

$$\langle v^n\rangle_t=\int_0^{2\pi}dx\int_{-\infty}^{\infty}dv\,v^nP(x,v,t)\,. \tag{13}$$

With the use of (6) they can be expressed as

$$\langle v^n\rangle_t=\lim_{k\to 0+}\left(i\frac{\partial}{\partial k}\right)^n a_0^t(k)\,. \tag{14}$$

We will consider in this paper the second moment which is related to the diffusion coefficient D by[1]

$$D=\lim_{T\to\infty}\frac{\langle(v-v_0)^2\rangle_T}{2T}\,. \tag{15}$$

Throughout this paper we assume the final time T to be a large integer $T\gg 1$.

II. PATHS IN FOURIER SPACE–ANALYTICAL CALCULATIONS

Starting from the initial Fourier amplitude a_m^0 we can find the final amplitude a_0^T as a product of T transitions. Every transition can be considered as a path in m, k space. In fact, we will go backward in time. Since we are interested in a_0^T $(k\to+0)$ [see Eqs. (14) and (15)], a path must start at the origin $m=0$, $k=+0$. The simplest path is one which never leaves the origin. It contributes

$$a_0^T(k)=[J_0(k\epsilon)]^T a_0^0(0)\,. \tag{16}$$

Then from (15) we find

$$D_{QL}=\frac{\epsilon^2}{4}, \tag{17}$$

where we have used the expansion of J_0 for small argument

$$J_0(k\epsilon)\approx 1-\left(\frac{k\epsilon}{2}\right)^2. \tag{18}$$

This simplest path corresponds to a value of diffusion given by quasilinear theory.[1,3]

Consider now paths which do leave the origin. According to Eqs. (10)–(12) an amplitude $a_m^t(k)$ may be connected by a single-path step to $a_{m'}^{t-1}(k')$ where (k',m') must lie on the vertical line $k'=k+m$. As a result of such a transition, the amplitude accumulates a factor of $J_l(|k'|\epsilon)\exp[-(\sigma/2)m^2]$. This simple geometrical rule, illustrated in Fig. 1, allows construction of all possible transition paths.

Note further that in leaving or returning to the origin, we obtain factors $J_l(k\epsilon)$. Since we are interested in the limit $k\to+0$, only $l=\pm1$ are of low enough order in k to contribute to the diffusion. It is also clear that we do not need to consider

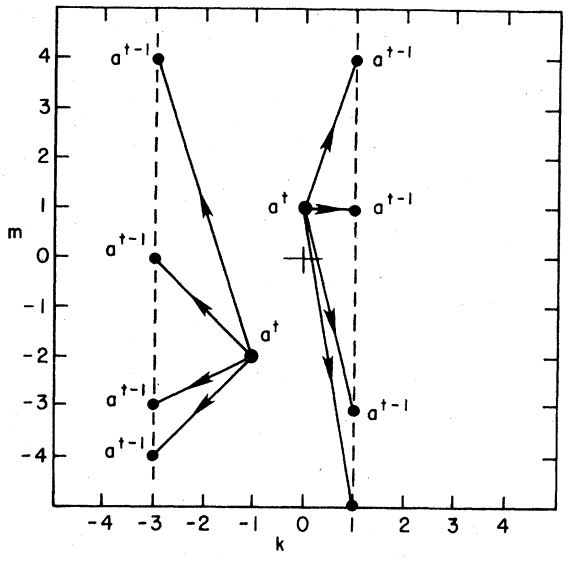

FIG. 1. Examples of path steps in Fourier space contributing to the probability amplitude. A single-path step can connect the point (k,m) to any point (k',m') with $k'=k+m$.

any paths which leave or return to the origin more than once (too high order in k). As an illustration of this method, we rederive and extend the main result of Ref. 1, Eq. (20), valid for large ϵ. As pointed out, we require $l=\pm1$ for the path steps leaving and entering the origin. Thus, a path must leave the origin through the point $(k,m)=\pm(0,1)$ and enter the origin through the point $\pm(1,-1)$. A step leaving the origin thus contributes a factor $J_{\pm1}(k\epsilon)$ and entering the origin contributes a factor $J_{\pm1}(k\epsilon)e^{-\sigma/2}$. These two steps produce a factor of k^2 in $a_0^T(k)$, and by Eq. (14) any additional factors of k will give zero contribution to the diffusion.

Recall that each step in the path accumulates an additional factor of a Bessel function, which is small for $\epsilon\gg1$ with the exception of factors $J_0(k\epsilon)$ obtained by remaining at the origin $(k\to0)$ for a step. Thus, for large ϵ we can construct a series in ascending powers of Bessel functions by considering paths with an increasing number of steps not spent at the origin. The path with the fewest number of steps spent outside the origin is constructed by connecting $(0,1)$ to $\pm(1,-1)$ in a single step, which can be done only as shown in Fig. 2(a):

$$(0,0)\to(0,1)\to(1,-1)\to(0,0)\,. \tag{19}$$

We refer to this as a first-order path. It can be traversed in T steps $T-2$ different ways, by remaining at the origin S steps before moving, with $S=0,1,2,\ldots,T-3$. The contribution of these $T-2$ paths to $a_0^T(k)$ is

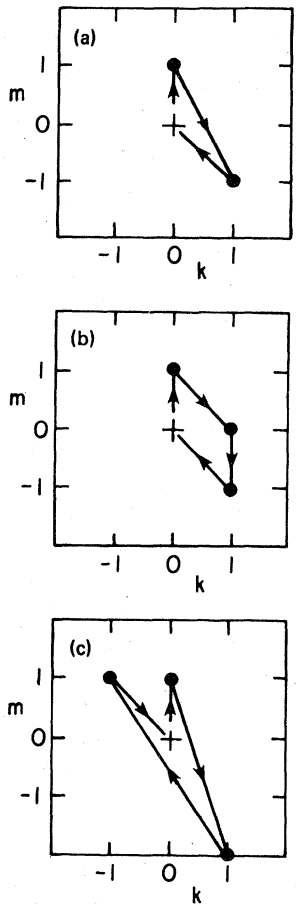

FIG. 2. Paths contributing to the diffusion for large ϵ. The first-order path (a) contributes the $J_2(\epsilon)$ term, and second-order paths (b) and (c) contribute the $J_1^2(\epsilon)$ and $J_3^2(\epsilon)$ terms, respectively. There is also one third-order path which contributes the $J_2^2(\epsilon)$ term of Eq. (26).

$$a_0^T(k) = (T-2)[J_0(k\epsilon)]^{T-3} J_{-1}(k\epsilon) J_{-1}(k\epsilon) \times e^{-\sigma/2} J_2[(1+k)\epsilon] e^{-\sigma/2} \tag{20}$$

which, from Eqs. (14) and (15), and using $J_1(k\epsilon) \sim (k\epsilon/2)$, contributes $(-\epsilon^2/4) J_2(\epsilon) e^{-\sigma}$ to the diffusion. There is an equal contribution from the path obtained by reflection through the origin. Now consider second-order paths, i.e., those involving two steps connecting (0, 1) to $\pm(1, -1)$. From (0, 1) the path can move only to points $(1, m)$. To complete the path we require from Eq. (11) that $m+1 = \pm 1$. The choice $m=0$ gives the path shown in Fig. 2(b):

$$(0,0) \to (0,1) \to (1,0) \to (1,-1) \to (0,0), \tag{21}$$

and a contribution to D of $(-\epsilon^2/4) J_1^2(\epsilon) e^{-\sigma}$. Again, there is an equal contribution from the reflected path. The choice $m=-2$ gives the path shown in Fig. 2(c):

$$(0,0) \to (0,1) \to (1,-2) \to (-1,1) \to (0,0), \tag{22}$$

which contributes to D the term $(\epsilon^2/4) J_3^2(\epsilon) e^{-3\sigma}$. Again, there is an equal contribution from the reflected path. Third-order paths are also easily obtained. The most general path involving three steps connecting (0, 1) to $\pm(1, -1)$ is given by

$$(0,0) \to (0,1) \to (1,m) \to (m+1,n) \to \pm(1,-1) \to (0,0) \tag{23}$$

with $m+n+1 = \pm 1$. The plus sign gives a contribution to D of

$$-\sum_{m=-\infty}^{\infty} \frac{\epsilon^2}{4} J_{1-m}^2(\epsilon) J_{2m}(|m+1|\epsilon) e^{-\sigma(m^2+1)}, \tag{24}$$

and the minus sign a contribution of

$$+\sum_{m=-\infty}^{\infty} \frac{\epsilon^2}{4} J_{1-m}(\epsilon) J_{2m+2}(|m+1|\epsilon) J_{m+3}(\epsilon) e^{-\sigma(m^2+2m+3)}. \tag{25}$$

Again, the reflected paths contribute equally. Note that the $m=-1$ term is only second order in Bessel functions. Similarly, fourth-order paths contribute some third-order Bessel terms, which are easily obtained. Finally, we find

$$\frac{D}{D_{QL}} = 1 - 2J_2(\epsilon)e^{-\sigma} - 2J_1^2(\epsilon)e^{-\sigma} + 2J_3^2(\epsilon)e^{-3\sigma} + 2J_2^2(\epsilon)e^{-2\sigma} - 2\sum_{m=-\infty}^{\infty} J_{1-m}^2(\epsilon) J_{2m}(|m+1|\epsilon) e^{-\sigma(m^2+1)}$$
$$+ 2\sum_{\substack{m=-\infty \\ m\neq -1}}^{\infty} J_{1-m}(\epsilon) J_{m+3}(\epsilon) J_{2m+2}(|m+1|\epsilon) e^{-\sigma(m^2+2m+3)} - 2J_2(\epsilon)J_3^2(\epsilon)e^{-4\sigma} - 2J_2(\epsilon)J_3^2(\epsilon)e^{-(9/2)\sigma}$$
$$+ 2J_1(\epsilon)J_2^2(\epsilon)e^{-2\sigma} + 2J_2(\epsilon)J_1^2(\epsilon)e^{-2\sigma}. \tag{26}$$

This result extends Eq. (20) of Ref. 1, which included only the first four terms.

Now consider the case $\epsilon \ll 1$. We utilize the fact that the Bessel functions $J_l(\epsilon)$ are proportional to ϵ^l when $\epsilon \ll 1$. As we will see later, only paths involving $l = 0, +1$ contribute to lowest order in ϵ. Consider a path represented in Fig. 3. It starts at the origin $(k, m) = (k, 0)$, $k \ll 1$, stays there for s transitions, then moves to an ending point $(p+k, 0)$, p integer (the case $p=3$ is depicted on Fig. 3), and then remains

T-s-p transitions at this point. The contribution from such a path for the case $p>0$ is equal to

$$a_0^T(k)=J_0^s(k\epsilon)J_{-1}(k\epsilon)\prod_{i=1}^{p-1}J_0[(i+k)\epsilon]\exp[-(\sigma/2)p]J_1[(p+k)\epsilon]J_0^{T-s-p}[(p+k)\epsilon]a_0^0(p+k)\,. \tag{27}$$

Path points on the k axis can remain stationary an arbitrary number of transitions, and we indicate these points with a cross. Factors $J_0^s(k\epsilon)$ give 1 in the limit $k\to 0$, and we will omit them in the following.

The diffusion is readily calculated to lowest order in ϵ for two limits, characterizing early and late times. For the early time limit assume that $p\epsilon\ll 1$ and $1\ll T\ll(2/p\epsilon)^2$ so that $J_0^{T-s-p}(p\epsilon)\approx 1$. Then with the use of the identity $J_{-1}(\epsilon)=-J_1(\epsilon)$ and $J_1(\epsilon)=\epsilon/2$, $\epsilon\ll 1$ we find

$$a_0^T(k)=-\frac{Tk(p+k)\epsilon^2}{4}\exp[-(\sigma/2)p-ipv_0]\,. \tag{28}$$

The factor of T in front of this equation comes from the summation over s. (Here we use $T\gg p$, the factor is acutally T-p-1.)

The case $p<0$ can be considered in a similar way. Using Eq. (15), and summing over all $p=\pm1,\pm2,\ldots$, we can obtain the contribution to D which we combine with expression (17) to find

$$D=\frac{\epsilon^2}{4}\frac{[1-\exp(-\sigma)]}{\{1-2\cos v_0\exp[-(\sigma/2)]+e^{-\sigma}\}}\,. \tag{29}$$

The approximate region of applicability of this formula is

$$1\ll T\ll(2/\epsilon)^2,\quad \sigma\gg\epsilon\,. \tag{30}$$

The class of paths represented by Fig. 3 is unique in that they involve only two factors of J_1 and no higher-order Bessel functions. It is easy to show that any modification of the path will produce additional $J_l(\epsilon)$ with $l>0$, and thus, will contribute to D only in a higher order of ϵ.

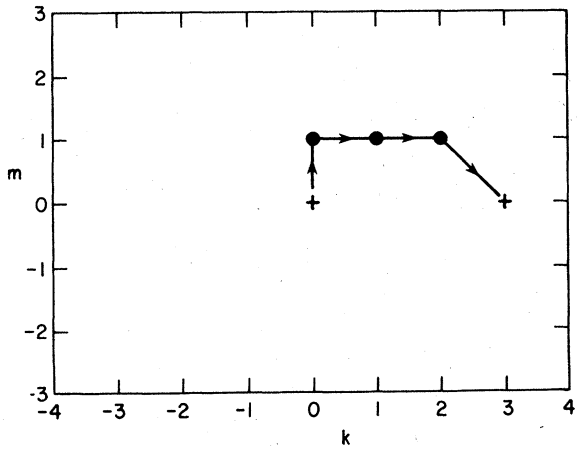

FIG. 3. An example of a multistep path in Fourier space. The crosses indicate points at which the path can remain for several steps.

Consider now the limit $T\gg(2/\epsilon)^2$. Then the factors $J_0^{T-s-p}(p\epsilon)$ in Eq. (19) are small. Owing to this, only paths which come back to the origin contribute. The simplest path of this type is shown in Fig. 4(a). Its contribution is equal to

$$a_0^T(k)=TJ_{-1}(k\epsilon)J_1(\epsilon)\exp[-(\sigma/2)]J_0^n(\epsilon)J_1(\epsilon)\times\exp(-\sigma/2)J_{-1}(k\epsilon)a_0^0. \tag{31}$$

Summing over all $n=0,1,2,\ldots$, we find

$$a_0^T(k)=T\left(\frac{k\epsilon}{2}\right)^2\frac{J_1^2(\epsilon)}{1-J_0(\epsilon)}e^{-\sigma}. \tag{32}$$

In the limit of $\epsilon\ll 1$ its contribution to the diffusion is equal to $-(\epsilon^2/4)\exp(-\sigma)$. The exact same value arises from a reflected path leaving the origin in a downward direction.

Let us now turn to a more complicated path, depicted on Fig. 4(b). Every crossing of a path with the abscissa at k_c gives a factor similar to that of Eq. (32):

$$\pm\frac{J_1^2(|k_c|\epsilon)}{1-J_0(|k_c|\epsilon)}\approx\pm 1,\quad k_c\epsilon\ll 1.$$

If we designate by k_R the last cross to the right different from the origin, then the number of possible crosses between the origin and that cross is $n_R=k_R-1\geq 0$. The same applies for the number of possible crosses between the origin and the last one to the left, $n_L=k_L-1\geq 0$. The total number of such crosses is

$$n=n_R+n_L\,. \tag{33}$$

In the case $n>0$, the contribution from any given path of the type from Fig. 4(b) is equal to

$$a_0^T(k)=(-1)^{d-2}T\left(\frac{k\epsilon}{2}\right)^2\exp[-\sigma(n+2)]\,. \tag{34}$$

Here d is the total number of diagonal lines on the path. It is easy to see that for a given n_R and n_L the total number of different paths which have a positive sign in Eq. (34) is equal to $\sum_{i=0}^{n}C_{2n}^{2i}$, while the number of paths with a negative sign is $\sum_{i=1}^{n}C_{2n}^{2i-1}$, where C_n^i is a binominal coefficient. Owing to the identity

$$\sum_{i=0}^{2n}C_{2n}^i(-1)^i=(1-1)^{2n}=0\,, \tag{35}$$

we have exact cancellation of contributions from

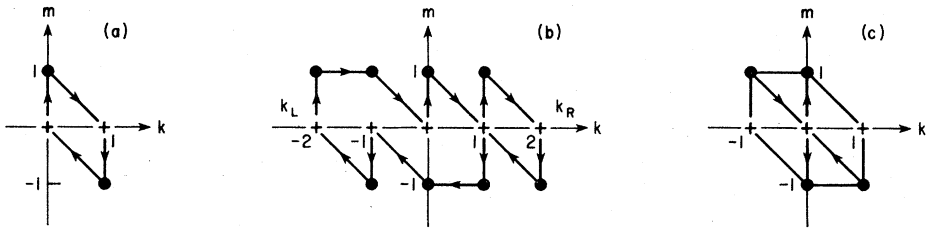

FIG. 4. Paths in Fourier space. They must leave the origin through the point $(k,m)=\pm(0,1)$ and return through $\pm(1,-1)$.

these paths. Thus, only paths with $n=0$ contribute. They are drawn on Fig. 4(c). It is straightforward to show that their contribution to the diffusion is given by

$$\frac{\epsilon^2}{4}(-1)^p e^{-p\sigma}, \quad p=1,2,3,\ldots . \tag{36}$$

Here the integer p corresponds to the number of half circles around the origin. Also the contributions from paths in clockwise and anticlockwise directions are equal. Summing over p and combining with Eq. (17), we can finally obtain, to lowest order in ϵ for $T \gg (2/\epsilon)^2$,

$$D/D_{QL} = \tanh(\sigma/2) . \tag{37}$$

To conclude this section we recall that D_{QL} can be derived by using the random-phase approximation,[1] i.e., assuming that the phase x becomes randomly distributed after each step. Thus, the deviation of D from D_{QL} represents the effect of phase memory. Also, the number of steps necessary to evaluate $D-D_{QL}$ corresponds to the characteristic time τ_c for the decay of this phase memory. In the case $\epsilon \gg 1$, $|D/D_{QL}-1| \ll 1$, is represented by the second term in Eq. (20), Ref. 1, and the phase memory decays in a few steps $\tau_c \sim 1$. On the other hand, if $\epsilon \ll 1$, $\sigma \ll 1$, $D \ll D_{QL}$, and a large number of steps ($\tau_c \sim 1/\sigma$) are necessary to calculate $D-D_{QL}$. Thus, the phase memory decays very slowly, as one would expect for nearly integrable systems.

III. NUMERICAL SUMMATION OF PATHS IN FOURIER SPACE

The analytical calculation of D/D_{QL} to higher order in ϵ involves the summation of a rather large set of paths in Fourier space, and we have carried out this summation numerically. From Eq. (10), we find that symmetry or antisymmetry of $a_m^t(k)$ under m, $k \to -m$, $-k$ is propagated from $t-1$ to t. Taking $a_m^0(k)$ as given by Eq. (7) with $V_0=0$, we thus have that $a_m^t(k)$ is symmetric under this reflection. We are interested in long-time behavior so the value of V_0 is irrelevant. We then need keep only $k \geq 0$. Now truncate in Fourier space through

$$\begin{aligned} &-M \leq m \leq M , \\ &0 \leq k \leq K , \end{aligned} \tag{38}$$

and replace (k,m) with the single index $n=(2M+1)k+m$ where $1 \leq n \leq N$, $N=(2M+1)K+M$. From the preceding analysis, we can take the path to originate by leaving the origin through $m=-1$, $k=1$, i.e., $a_n^1=\delta_{n,2M}\exp(-\sigma/2)$. (We are now following the path forward in time, i.e., backwards along the arrows of Fig. 2.) The term $a_0^t(0)$ is excluded since the paths considered return to the origin only once, passing through $(k,m)=(0,1)$. The diffusion is given by

$$\frac{D}{D_{QL}} = 1-2A_1 , \tag{39}$$

where $A_1=\lim_{t\to\infty} a_1^t$, since the path must terminate by entering the origin through $(k,m)=(0,1)$. From Eq. (10), the vector A satisfies the matrix equation

$$A=(1+B+B^2+\cdots)a^1=(1-B)^{-1}a^1 , \tag{40}$$

where

$$B_{ij}=\exp[-(m^2\sigma/2)][J_{m-m'}(k'\epsilon)\delta_{k',m+k} - J_{-(m+m')}(k'\epsilon)\delta_{k',-m-k}] , \tag{41}$$

with

$$m=\begin{cases} i \bmod(2M+1), & i \bmod(2M+1) \leq M \\ i \bmod(2M+1)-(2M+1), & i \bmod(2M+1) > M \end{cases} \tag{42}$$

$$k=\frac{i-m}{2M+1} \tag{43}$$

and similar equations relating m', k' to j. Gaussian elimination is then used to find the diffusion through Eq. (39). As numerical checks on this method, we used the trivial case $M=1$, $K=1$, for which B_{ij} is 4×4, as well as confirming that for $\epsilon \ll 1$, $\sigma \ll 1$ the case $M=1$, $K \gg 1$ converges for

large K to the partial result

$$\frac{D}{D_{QL}} = \tanh\frac{\sigma}{2} + \frac{3\epsilon^2}{16\pi^2}, \tag{44}$$

obtained by summing all paths restricted within $-1 \leq m \leq 1$. Equation (44) is not a correct expression for D/D_{QL} to order ϵ^2; paths with excursions out to $m = \pm 2$ cancel this ϵ^2 term. In addition, we have compared this method to results obtained by numerically advancing the Chirikov-Taylor mapping for values of ϵ and σ for which this is practical. We have not been able to analytically derive the lowest-order corrections (in ϵ) to Eq. (37). The numerical results indicate that these corrections are not analytic in σ. These results are discussed in Sec. IV.

IV. NUMERICAL RESULTS FOR SMALL ϵ

We turn now to the results of numerical computations. Two methods have been used. First, where practical, we have calculated the diffusion directly through Eq. (15) by advancing Eqs. (1) and (2) with the introduction of a random step in x having a normal distribution of variance σ. A large number of particles N_p is used, due to the presence of fluctuations in D proportional to $N_p^{-1/2}$. Full advantage of the vector processing capabilities of the MFE CRAY 1 have been used, but it is still not practical to obtain values for the diffusion in this manner when both ϵ and σ are quite small. Approximately, 2 μsec of cpu time is necessary per particle step. Figure 5 shows the ratio of D to the quasilinear value as a function of σ for $\epsilon = 0.06$, and two values of V_0. Each point is obtained by advancing 1000 particles initially distributed uniformly in x at $V = V_0$. For values of T such that $1 \ll T \ll (2/\epsilon)^2$, the observed values agree with the analytical result given by Eq. (29), shown with a solid curve. Also shown is the result for $T \gg (2/\epsilon)^2$ when the particles have diffused sufficiently far in phase space that the initial correlations associated with the value of V_0 have been lost. The diffusion is then seen to be described by Eq. (37). We have also investi-

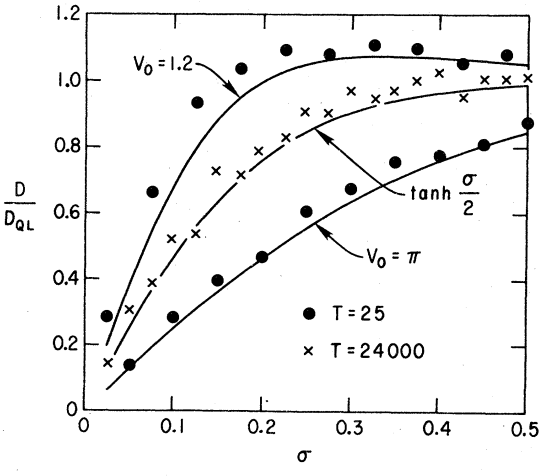

FIG. 5. The ratio of the diffusion to the quasilinear value as a function of σ obtained using the Chirikov-Taylor mapping. The particles were initially uniformly distributed in x and located at $V = V_0$. For $1 \ll T \ll 2/\epsilon^2$ the results agree with Eq. (29), whereas for $T \gg 2/\epsilon^2$, the diffusion is given by Eq. (37). Here $\epsilon = 0.06$.

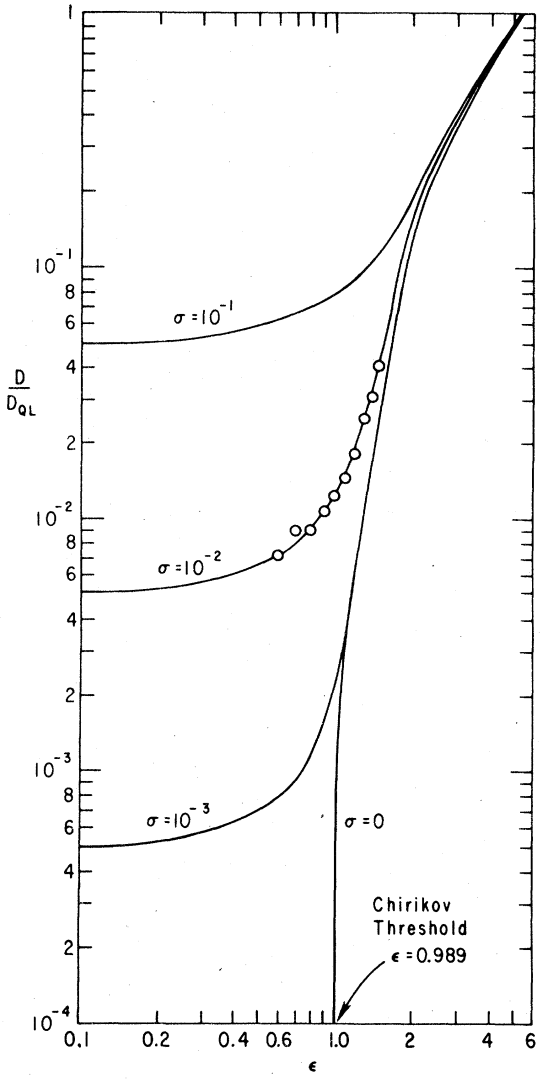

FIG. 6. The diffusion as a function of ϵ for small ϵ and various values of σ. The points were obtained using the Chirikov-Taylor mapping directly, and the curves by the path-summation technique of Sec. IV. For $\sigma = 0$, the diffusion vanishes for ϵ less than the Chirikov threshold value.

gated the small-ϵ and small-σ regime. Results obtained by advancing Eqs. (1) and (2) to $T = 29\,000$ are shown in Fig. 6. We have used this method for $0.6 < \epsilon < 1.5$. At small ϵ large times are necessary to obtain convergent results due to the very small rates of diffusion, and for $\epsilon < 0.6$, it is prohibitive to find the correction to Eq. (37) in this manner. At $\epsilon = 0.7$, for example, the diffusion approaches its asymptotic limit as

$$\frac{D}{D_{QL}} = \left(\frac{D}{D_{QL}}\right)_{\text{asym}} + \frac{40}{T}, \tag{45}$$

for the initial conditions used. Here we have used 2000 particles initially distributed uniformly in x for $0 \leq x \leq 2\pi$ and randomly in V for $0 \leq V \leq 2\pi$. A detailed investigation of the dependence of D on σ and ϵ is not feasible, and $\sigma = 10^{-2}$, $\epsilon = 0.5$ is practically the lower bound. Each point on Fig. 6 required approximately two minutes of cpu time, and the results, of course, still include statistical error. Reducing the error to 1% for the point $\epsilon = 0.7$ would by Eq. (45) require one-half hour of cpu time.

To complement these results, we have used the numerical path-summation technique discussed in Sec. III. Figure 7 shows the dependence of the numerical results on the Fourier-space truncation parameters M, K, for ϵ below the Chirikov threshold.[2] For fixed M convergence is seen to proceed stepwise in $1/K$, indicating the existence of critical scale lengths in phase space for contributions to a particular order in ϵ. The values $K = 30$, $M = 10$ result in a 640×640 dimensional matrix B_{ij}, which is approximately the computational upper bound. A determination of the diffusion requires approximately two minutes of CRAY time with M, K this large, and the practical ranges of ϵ, σ are significantly extended over what is possible by directly using the Chirikov-Taylor mapping. For $\epsilon > 1$, except in the vicinity of $\epsilon = 2\pi$, much smaller values of K, M suffice to give convergent results. The large extent in Fourier space of the contributing paths undoubtedly indicates that for $\epsilon < 1$ the diffusion is spatially localized, perhaps into filaments attached to separatrices. In Fig. 6 are shown the results obtained in the small-ϵ regime for different values of σ. The $\sigma = 0$ results are consistent with the vanishing of the diffusion below the Chirikov limit. These results are seen to agree quite well with those obtained by stepping Eqs. (1) and (2). As shown in Fig. 7, $M = 5$, $K = 20$ are sufficient to obtain convergent results at $\epsilon = 0.5$, $\sigma = 10^{-2}$. This corresponds to a matrix of dimension 225×225 and a saving of approximately a factor of 4 in cpu time over direct use of the mapping. More significant is the large extension of the domain of possible values of ϵ, σ provided by the path summation technique, as shown in Fig. 6. The path-summation method converges for small ϵ and $\sigma = 10^{-3}$ with sufficient accuracy to determine the correction to Eq. (37), requiring two minutes of cpu time. It is clear from the discussion following Eq. (45) that determination using the direct mapping would require hours of cpu time.

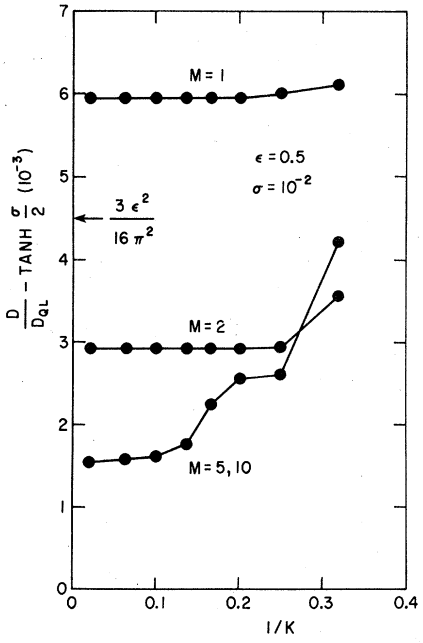

FIG. 7. The convergence of the Fourier path-summation method. Shown are values of $(D/D_{QL}) - \tanh \sigma/2$ as a function of $1/K$ for various M. Here $\epsilon = 0.5$ and $\sigma = 10^{-2}$. As $\epsilon \to 0$ and $\sigma \to 0$, the $M = 1$ curve is found to converge to the value $(3\epsilon^2/16\pi^2)$.

Figure 8 shows the correction to the lowest-order expression for D given by Eq. (37). Determination of this correction below $\epsilon = 0.5$ is not numerically feasible with the present schemes. Assuming the corrections to be of the form of even powers in ϵ, a result expected by the nature of terms appearing in the path summations, we find that these results are reasonably well fit by

$$\frac{D}{D_{QL}} = \tanh\left(\frac{\sigma}{2}\right) + a\sigma^{2/3}\epsilon^2 + b\epsilon^4, \tag{46}$$

with $a \approx \frac{1}{8}$ and $b \approx 2 \times 10^{-3}$. The dependence of b on σ cannot be determined from the data available, except that it must be quite weak. Of course, b must vanish as $\sigma \to 0$.

Figure 9 shows D/D_{QL} for $0 < \epsilon < 20$, and $\sigma = 10^{-3}$ obtained with the numerical Fourier path-summation technique. We find that large M, K is necessary to observe the peak at $\epsilon \approx 2\pi$, where D be-

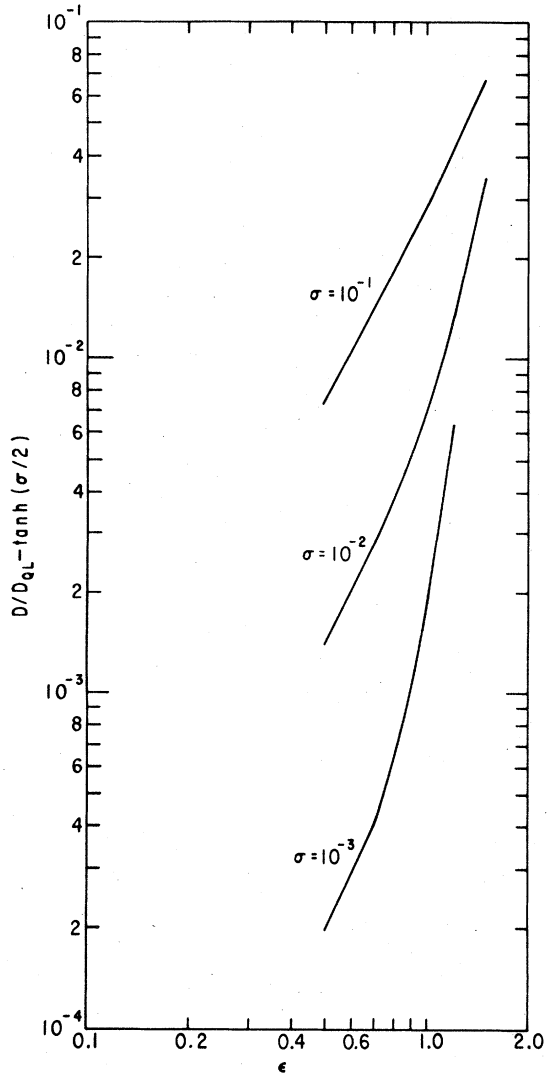

FIG. 8. Corrections to Eq. (37) as a function of ϵ for various σ, obtained using the Fourier path-summation method.

comes more than three times the quasilinear value for this value of σ. Chirikov[2] has pointed out the existence of acceleration $D \to \infty$ as $\sigma \to 0$. In regular motion for $\epsilon \approx 2\pi n, n$ interger. Particles within these islands move according to $V = V_0 + t$. Owing to this acceleration $D \to \infty$ as $\sigma \to 0$. In fact within these domains the particles stream rather than diffuse, and thus the diffusion coefficient D becomes infinite as $\sigma \to 0$. Further analysis of this behavior will be reported in a future publication.[4] Also shown is the analytic expression for large ϵ derived in Ref. 1.

V. CONCLUSION

Determination of the time evolution of the solution of the Vlasov equation through the method of paths in Fourier space greatly extends the results obtainable through direct stepping of the Chirikov-Taylor mapping. The method provides lowest-order closed-form analytic expressions for the diffusion, and the means of calculating to higher order numerically. We believe that it will prove useful in the examination of other problems involving chaotic or turbulent dynamics.

ACKNOWLEDGMENTS

We would like to acknowledge valuable conversations with J. Greene and C. Oberman, and valuable numerical assistance from M. Petravic. We are also thankful to T. Antonson and R. Cohen for pointing out inaccuracies in our paper. This work was supported by United States Department of Energy Contract Nos. DE-AC02-76-CH03073 and DE-AS02-78ET53074.

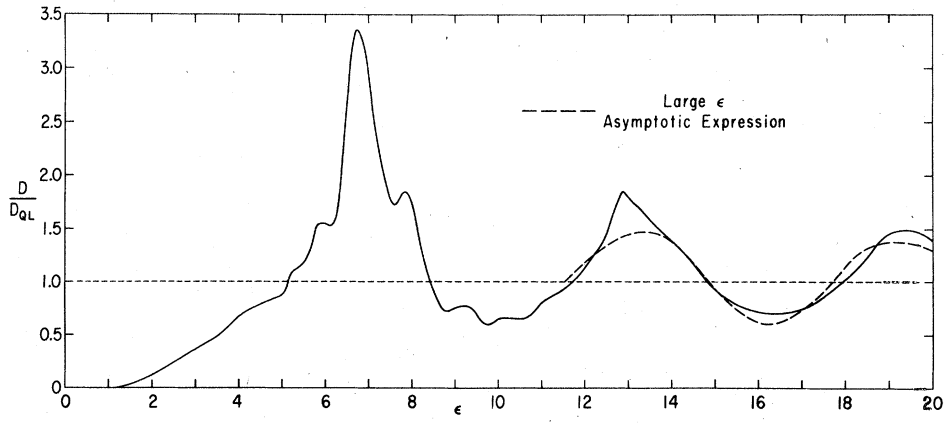

FIG. 9. The ratio of D/D_{QL} as a function of ϵ for $0 < \epsilon < 20$, as obtained using Fourier path summation. The peak at $\epsilon \approx 2\pi$ is associated with paths with large extent in (m,k) space. Also shown is the large-ϵ expression. Here $\sigma = 10^{-3}$.

*Present address: The Institute for Fusion Studies, University of Texas, Austin, Texas.

[1]A. B. Rechester and R. B. White, Phys. Rev. Lett. 44, 1586 (1980).

[2]B. V. Chirikov, Phys. Rep. 52, 263 (1979).

[3]G. M. Zaslavsky and B. V. Chirikov, Usp. Fiz. Nauk 14, 195 (1972) [Sov. Phys.—Usp. 14, 549 (1972)].

[4]C. F. Karney, A. B. Rechester, and R. B. White, Bull. Am. Phys. Soc. 25, 996 (1980), paper 8F2.